

BORON CONCENTRATION MEASUREMENTS AT THE I/P INTERFACE IN NIP A-SI SOLAR CELLS

B.B. Van Aken¹, M. Duchamp², C.B. Boothroyd², R.E. Dunin-Borkowski³, J-P Barnes⁴, M Veillerot⁴ and W.J. Soppe¹

¹ECN Solar Energy, P.O. Box 1, NL-1755 ZG Petten, the Netherlands

²Center for Electron Nanoscopy, Technical University of Denmark, DK-2800 Kongens Lyngby, Denmark

³Institute for Microstructure Research, Forschungszentrum Jülich, D-52425 Jülich, Germany

⁴CEA-Leti, MINATEC Campus, 17 rue des Martyrs, FR-38054 Grenoble Cedex 9, France

Phone: +31 224 564905; Fax: +31 224 568214; email: vanaken@ecn.nl

ABSTRACT: The p-type Si layer in n-i-p a-Si and μ c-Si solar cells on foil has several important requirements with respect to conductivity and optical transmission. We control the optical band gap and activation energy of p-a-SiC by varying the B₂H₆ and CH₄ flows in the process chamber. Modelling shows that the optimum efficiency in n-i-p solar cells is obtained when the p-a-SiC band gap is just above the band gap of the absorber layer. We have assessed the potential of core-loss electron energy-loss spectroscopy (EELS) for detecting B and C and of low-loss EELS, in a spatially resolved manner, as probe of local variations in bulk plasmon energy. EELS in the transmission electron microscope (TEM) combines the necessary spatial resolution to investigate the boundary between p-a-SiC and i-a-Si with sufficient sensitivity to the boron content.

Keywords: amorphous and microcrystalline Si, thin film solar cells, boron concentrations using core-loss EELS, TEM, bulk plasmon energy using EELS

1 INTRODUCTION

Roll-to-roll production of thin film Si solar cells has several advantages over batch-type reactor systems, for instance high-throughput fabrication and the opportunity to make lightweight and flexible products. Flexible and lightweight PV modules gear up to building integrated PV: the most important market for PV in densely populated, developed countries [1, 2]. ECN is developing a concept for roll-to-roll production of high efficiency n-i-p solar cells based on amorphous (a-Si:H) and microcrystalline (μ c-Si:H) silicon thin films on steel foil coated with an insulating barrier layer and sputtered back contact and reflection layer.

The p-type Si layer in n-i-p a-Si and μ c-Si solar cells on foil has several important requirements. The layer is necessary to create the electric field that separates the photo-generated charge carriers; the doping also increases the conductivity to conduct the photocurrent to the front contact; on the other hand, the p-layer should transmit the incident light efficiently to the intrinsic absorber layer. To obtain good conductivity, the typically required B concentration is $\sim 10^{21}$ cm⁻³ in the thin p-a-Si layer, but should be below 10^{17} cm⁻³ in the adjacent intrinsic absorber layer [3]. To increase the amount of transmitted light through the p-doped Si layer, this layer is typically alloyed with C (referred to as p-a-SiC).

To make high efficiency Si solar cells, it is very important to control and limit the diffusion of B and C atoms into the i-layer during the following layer deposition and processing of the solar cells. SIMS profiles have been realised on flat solar cells. These solar cells show an improved efficiency when the B contamination is kept low in the i-layer. However, the i/p interface has an average roughness of ~ 10 nm, which is about the thickness of the p-layer (Figure 2), thus making accurate determination of the B profile at the i/p interface impossible with SIMS. In that case, electron energy loss spectroscopy (EELS) in the transmission electron microscope (TEM) may combine the necessary spatial resolution to investigate the boundary between p-a-SiC and i-a-Si with sufficient sensitivity to the boron content and the carrier concentration. EELS-TEM is a spectrometric technique which allows measuring the

energy loss of an electron beam when travelling through the TEM specimen (see Figure 3). The physical processes involved in energy-loss can be (i) band gap transition, (ii) plasmon collective oscillation and (iii) interatomic transition. Therefore, they can provide information on (i) the band gap energy, (ii) the carrier density (through the plasmon energy, see eq. 2) and (iii) the local atomic composition with a nanometre range spatial resolution.

2 EXPERIMENTAL DETAILS

2.1 Sample fabrication

For EELS in the TEM, dedicated test samples of p-type SiC layers with a variation in B content are grown in the Flexicoat300. This roll-to-roll PECVD system allows growing n-i-p thin film Si solar cells on foils with a width up to 300 mm. The Flexicoat300 contains three inline vacuum chambers which are equipped with linear RF plasma sources for deposition of n- and p-type layers and with a linear VHF plasma source for deposition of intrinsic silicon layers.

The test samples consist of three ~ 200 nm SiC layers with no (i-SiC), standard (p+-SiC) and double (p++-SiC) amounts of B doping. To illustrate this, SIMS profiles of the B concentration are given in Figure 1. To estimate the relative B concentration obtained by SIMS, we assume that the total density of atoms is 5×10^{22} cm⁻³. For comparison also a standard a-Si solar cell is shown with a ~ 10 nm thick p-SiC window layer. Single p-type SiC layers are grown on glass and wafer substrates to facilitate standard characterisation of optical and electrical properties.

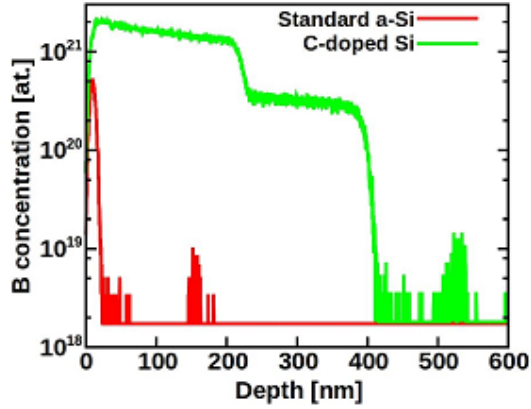


Figure 1: Boron concentration profiles by SIMS measurements of a n-i-p a-Si solar cell (red) and of the SiC test samples with three levels of p-type doping (green).

2.2 Electrical and optical characterisation

The optical and electrical properties of p-a-SiC are investigated by varying both diborane (B_2H_6) and methane (CH_4) flows during the deposition. Layers are characterised by the dark conductivity σ_d , its activation energy E_{act} determined by an Arrhenius fit of the temperature dependency

$$\sigma_d = \sigma_0 e^{(-E_{act}/kT)}, \quad (1)$$

and the optical band gap E_{04} , the photon energy at which the absorption coefficient $\alpha = 10^4 \text{ cm}^{-1}$.

2.3 Electron microscope

Thin film silicon solar cells, made on plastic, glass or metallic substrates, make sample fabrication for TEM difficult due to the different milling rate of the substrate compared to the active layer of the solar cell itself. 100 nm thick and 5 μm wide TEM lamellae have been prepared by focussed ion beam (FIB), the final milling step has been made with a 5 keV Ga^{2+} beam. A bright-field (BF) TEM image of the solar cell sample is shown in Figure 2a. In order to enhance the contrast from the SiC region, a thickness over lambda map is shown in Figure 2b. The p-layer, between the ITO and the i-Si layers, appears to have a dark contrast in Figure 2b due to the lower density of the p-SiC compared to the i-Si.

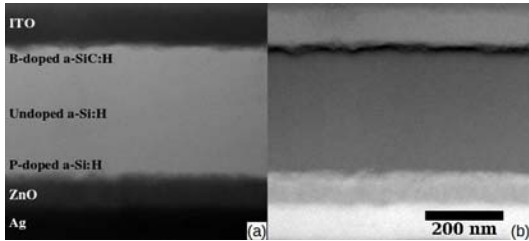


Figure 2: (a) Bright field and (b) thickness over lambda TEM image of an a-Si solar cell prepared using focus-ion-beam milling.

EELS has been performed on a FEI Tecnai T-20 equipped with a LaB_6 electron source and, when higher spatial resolution was needed on a FEI Titan 80-300 equipped with a field emission electron source, and a Gatan Tridiem imaging filter. Spectra were acquired in TEM-diffraction mode. All data taking was carried out at 120 keV to limit damage of the sample by the electron

beam. Figure 3 shows a typical EEL spectrum, indicating the plasmon loss region and the core-loss region.

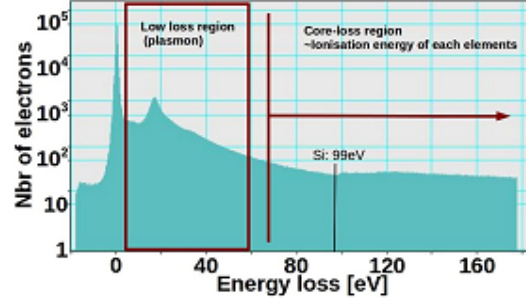


Figure 3: Typical EELS spectrum highlighting the relevant regions.

The core-loss EELS data have been averaged and background subtracted to isolate the B peak. For each area, 6 EELS spectra shifted in energy were acquired. Channel to channel gain variations were reduced using the iterative averaging process described in detail elsewhere [4]. To minimise the shot noise, the exposure time was kept as high as possible without damaging the specimen. For the large area measurements, each spectrum was acquired for one minute with a beam diameter of about 200 nm. For higher spatial resolution, line scans were made with a 5 nm beam in TEM diffraction mode. Each spectrum was acquired for 1.5 s. Details of the method are given elsewhere [5].

The low-loss EELS data have been acquired in scanning TEM. The bulk plasmon energies have been calculated by subtracting the energies obtained by fitting the bulk plasmon and the zero loss peaks. The bulk plasmon energy (E_p) is linked to the valence electron density according to:

$$E_p = \hbar \sqrt{\frac{ne^2}{\epsilon_0 m_0}}, \quad (2)$$

where n is the valence carrier density, e the elementary charge, ϵ_0 the permittivity of the free space and m_0 the effective mass.

3 RESULTS and DISCUSSION

3.1 Effect of boron and carbon doping

The electrical and optical properties of p-a-SiC are mainly determined by the amounts of (active) B and C present in the layer. In our case, B increases the conductivity of a-Si up to $\sigma_d > 10^{-3} \text{ S/cm}$ but also increases the absorption of photons by decreasing the E_{04} to $\sim 1.6 \text{ eV}$. In contrast, alloying intrinsic a-Si with C increases the E_{04} to $\sim 2.4 \text{ eV}$ and decreases the σ_d far below 10^{-10} S/cm .

First, we varied the flow rates of B_2H_6 and CH_4 , whilst keeping the other process conditions constant for a series of samples. Figure 4 shows the measured E_{04} and E_{act} of these samples. As expected, increase of CH_4 or decrease of B_2H_6 has the same effect, i.e. the E_{act} increases (σ_d decreases) and the E_{04} increases. Furthermore, we have found evidence for a linear relation between the E_{act} and the E_{04} for this set of p-a-SiC samples. The data point of C-free p-a-Si would be in the left corner, with $E_{act} < 0.3 \text{ eV}$ and $E_{04} \sim 1.6 \text{ eV}$.

Although the two elements B and C have opposite effects, they don't cancel each other completely. The

optimum combination of good conductivity and high band gap is obtained at the lowest amount of addition to the a-Si process.

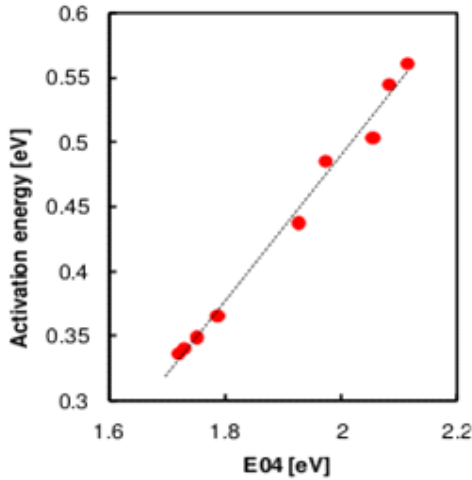


Figure 4: Relation between E_{act} and E_{04} data, obtained by varying the B_2H_6 and CH_4 flow rates. The dashed line is a linear fit to the data.

3.2 Modelling of p-a-SiC window layer

We have modelled a series of solar cells with ASA [6] to resolve the competition between transmission (high band gap) and conductivity (low activation energy).

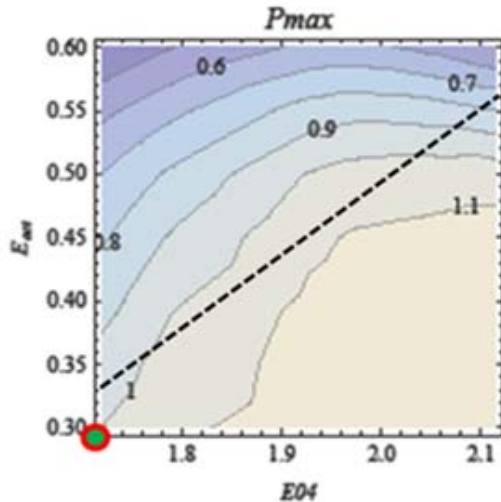


Figure 5: P_{max} as a function of E_{act} and E_{04} of the p-a-SiC layer, relative to the η calculated at $E_{act} = 0.30$ eV and $E_{04} = 1.7$ eV (indicated by the dot). The dashed line represents the, according to our measurements, experimentally accessible p-a-SiC.

As seen in Figure 5, the efficiency P_{max} falls strongly for $E_{act} > 0.5$ eV. Also for the lower E_{04} area with intermediate E_{act} values, a lower efficiency is found. Looking at the experimentally obtained data points, indicated by the dashed line, the optimum efficiency is found for a p-layer with an optical band gap of ~ 1.9 eV, just above that of the intrinsic layer. The activation energy is for that point just lower than 0.5 eV, in good agreement with published device quality values [7].

3.3 Core-loss EELS

We studied the B and C concentration profiles using core-loss EELS TEM. Experimental and calculated background subtracted B K-edge EEL spectra measured from the SiC test sample containing different B concentrations are shown in Figure 6a. The B peak of the highly doped sample is clearly recognisable and fits well with the simulated B peak after adjusting the crystallinity and the cluster size. As the B peak is quite narrow, we used an 8eV integration windows to estimate the area below the curves. The composition has been estimated by using the Hartree-Fock cross-section and is shown in insert of the Figure 6a. For comparison, we show the concentrations measured by SIMS on the same sample. For the undoped layer, no significant B concentration was measured by EELS. The B concentration of the p-a-SiC window layer in our standard solar cells, measured both using EELS and SIMS is 0.6 at. %.

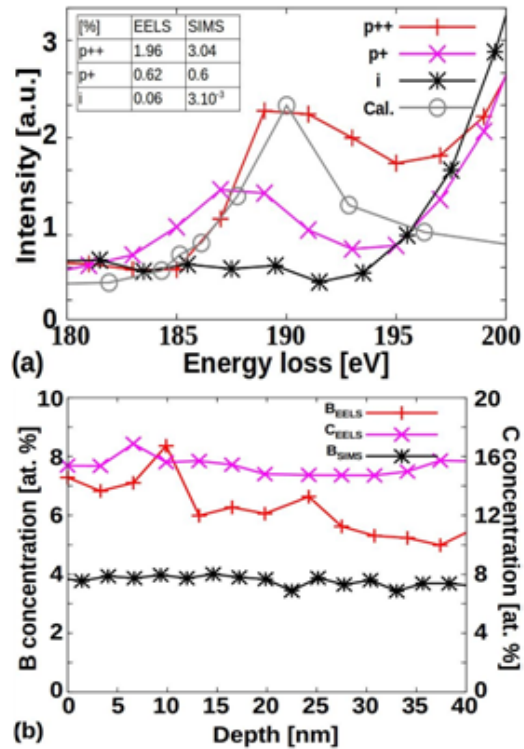


Figure 6: (a) Background subtracted core-loss EELS of the SiC stack with three different B concentrations. Insert: estimation of the B concentration calculated from the area below the curve. SIMS values have been obtained on the same sample. (b) B and C concentration profiles measured by TEM-EELS with a 5 nm probe. The B concentration profile measured by SIMS is shown for comparison.

Figure 6b shows the B concentration in the a-SiC layer close to the ITO interface, measured with SIMS and with EELS applying a 5 nm beam diameter. A slightly higher B concentration has been measured by EELS when compared to the SIMS profiles. This could be explained by the fact that data averages over a large area are obtained by SIMS.

3.4 Plasmon-loss EELS

We have used low-loss EELS to measure changes in plasmon energy and assess whether these changes are associated with active dopant concentration variations. The plasmon energy has been determined by the method described in section 2.3. In Figure 7, the plasmon energy has been plotted as a function of depth, measured from the ITO/p⁺⁺-SiC interface. We clearly observe a strong relation between B concentration and plasmon energy. By assuming that the density and the carrier mobility is independent of the B-doping level, we can consider that the increase of B concentration increases the valence electron density. Furthermore, the two outer data points, which are taken (partially) on the TCO front and back contacts, also exhibit high plasmon energies.

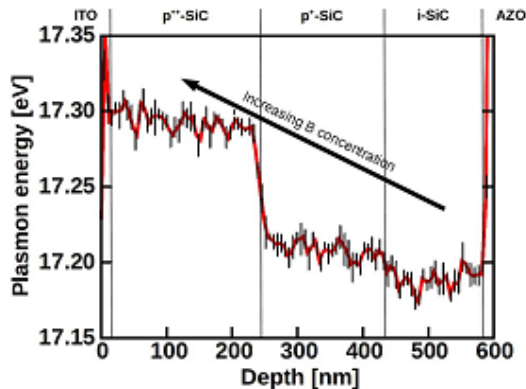


Figure 7: Plasmon energy as a function of depth relative to the ITO/p⁺⁺-SiC interface. The dashed lines represent the locations of the interfaces.

4 CONCLUSIONS

We control the band gap and activation energy of p-a-SiC by varying the B₂H₆ and CH₄ flow in the process chamber. A linear relation between the experimentally observed combinations of E_{act} and E₀₄ is found. Modelling shows that the optimum efficiency in n-i-p solar cells is obtained when the p-a-SiC band gap is just above the band gap of the absorber layer and E_{act} is still <0.50 eV.

We have assessed the potential of core-loss electron energy-loss spectroscopy (EELS) for detecting B and C concentrations as low as 10²⁰ cm⁻³, in solar cell-like devices. As proof of concept, we measured the B-concentration in a 200 nm thick layer with a 5nm beam probe. In both cases, the absolute concentrations are in reasonable agreement with the SIMS measurements. Such development offers the possibility to extend the EELS-TEM technique to real solar cells which have a 10 nm thick B-doped layer. The advantage of EELS-TEM is that the concentration is not averaged across the lateral directions, as is the case with SIMS. This allows to measure with EELS-TEM the B concentration profile of thin film with rough interfaces, particularly important when textured interfaces have been applied. Finally, low-loss EELS has been applied to probe the local variations in plasmon energy. This gives an independent tool to investigate the local modifications of the band structure.

ACKNOWLEDGEMENTS

This work has been financially supported by the EU (Silicon-Light project EU FP-7 Energy 2009-241477).

REFERENCES

- [1] M. Izu and T. Ellison, *Sol. Energy Mater. Sol. Cells* **78** (2003) 613.
- [2] A. Takano and T. Kamoshita, *Jpn. J. Appl. Phys.* **43** (2004) 7976.
- [3] U. Krol, et al., *Thin Solid Films* **451** (2004) 525.
- [4] C. B. Boothroyd, K. Sato and K. Yamada, *Proc. XIIth Int. Congress for Electron Microscopy*, p. 80 (1990).
- [5] M. Duchamp et al., *J. Phys. Conf. Series* (2011) submitted.
- [6] M. Zeman et al., *Amorphous Semiconductor Analysis (ASA)*, Delft University of Technology, the Netherlands, (2005).
- [7] R.E.I. Schropp and M. Zeman, *Amorphous and Microcrystalline Silicon Solar Cells – Modelling, Materials and Device Technology*, Kluwer Academic, Dordrecht, the Netherlands, (1998).